Supplementary Information for

Nanocomplex Made of Antimicrobial Metallo-Supramolecule And Model Biomembranes – Characterization and Enhanced Fluorescence

*Chung-Hao Liu[a], Heng Wang[b], Lin Yang[c], Yun Liu[d,e], Xiaopeng Li[b], Mu-Ping Nieh[a,f]**

[a]Polymer Program, Institute of Material Science, University of Connecticut, Storrs, Connecticut 06269, United States

[b]College of Chemistry and Environmental Engineering, Shenzhen University, Shenzhen 518055, China

[c]National Synchrotron Light Source – II, Brookhaven National Laboratory, Upton, NY, United States

[d]Center for Neutron Research, National Institute of Standards and Technology, Gaithersburg, Maryland 20899, United States

[e]Chemical & Biomolecular Engineering Department, University of Delaware, Newark, Delaware 19716, United States

[f]Department of Chemical and Biomolecular Engineering, University of Connecticut, Storrs, Connecticut 06269, United States

EXPERIMENTAL METHODS

Materials. 1,2-dipalmitoyl-*sn*-glycero-3-phosphocholine (DPPC), 1,2-dihexanoyl-*sn*-glycero-3-phosphocholine (DHPC), 1,2-dipalmitoyl-*sn*-glycero-3-phospho-(1'-rac-glycerol) (sodium salt) (DPPG),1,2-dihexanoyl-d_{22}-sn-glycero-3-phosphocholine-1,1,2,2-d_4-N,N,N-trimethyl-d_9 (DHPC-d_{35}) and 1,2-dipalmitoyl-d_{62}-sn-glycero-3-phosphocholine (DPPC-d_{62}) were purchased from

Avanti Polar Lipids (Alabaster, AL) and used without further purification. Dimethyl sulfoxide-d_6 (deuterated DMSO) was purchased from Cambridge Isotope Laboratories. The hexagonal prism supramolecules, **HP**, were synthesized in DMSO at 80 ^{o}C for 12 hours with the stoichiometric ratio of ligand/metal = 2/5, as described in the literature.[1]

Bicelles-supramolecular complex preparation. Pristine aqueous bicelle solution was made of three lipids, DPPC, DPPG and DHPC at a constant long-to-short chain molar ratio, [DPPC]+[DPPG])/[DHPC] = 3, and charged-to-total-long-chain lipid molar ratio, [DPPG]/([DPPC]+[DPPG]) = 0.05.[2] For **HP**-loaded samples, **HP** was first dissolved in chloroform/methanol mixture with a volume ratio of 1/3. The solution was added into appropriate amount of DPPC, DPPG and DHPC with different **HP**-to-lipid molar ratios of 1:3140 and 1:1047. Chloroform was evaporated by a stream of nitrogen on the hot plate. The **HP**/bicelle solutions were further dried under vacuum overnight to make sure chloroform was totally removed. Samples were then dispersed in water or null-contrast D_2O/H_2O to make the initial lipid concentration of 10 wt. %, which allows a reversible *T*-cycling (between 4 and 50 C) process until the final products were liquid-like. The solution is transparent at lower temperature (< 30 ^{o}C) but viscous at higher temperature (< 35 ^{o}C). The **HP**-loaded bicellar solutions then were further diluted at room temperature to a final lipid concentration of 1.0 or 0.1 wt.% for scattering and DSC measurements, respectively.

Encapsulation efficiency. Five different concentrations of free **HP** in MeOH/$CHCl_3$alone were prepared and measured by UV-vis absorption (PerkinElmer Lambda 1050) from 250 nm to 800 nm, yielding a calibration curve. The **HP**- loaded bicelles aqueous solution was diluted to 0.1 wt.% lipids concentration and centrifuge at 10,000 rpm (167 Hz) for 30 minutes to remove non-encapsulated **HP**. Both supernatant and precipitates were dried under nitrogen and redispersed according with mixture of chloroform and methanol. Then, the supernatant and precipitates were

conducted by UV-vis spectrometer at 285 nm. As a result, the amount of **HP** inside the bicelles can be obtained. The encapsulation efficiency can be expressed as[3,4]

$$EE(\%) = \frac{Total\ \ added\ HP\ (mg) - non\ encapsulated\ HP\ (mg)}{Total\ added\ HP\ (mg)} \times 100\%$$

Fluorescence Spectroscopy. The **HP**-loaded lipid sample was diluted to 0.1 wt.% lipids concentration and centrifuge at 10,000 rpm (167 Hz) for 30 minutes. The supernatant was loaded in quartz cells and measured by Fluorolog HORIBA Scientific with excitation wavelength 320 nm. The range of wavelength is from 400 nm to 610 nm.

Transmission electron microscopy (TEM). The TEM images were acquired by using FEI Tecnai T12 with accelerating voltage 80 kV. The bicelles and **HP**-loaded bicellar solution were dropped 3 μL with 0.002 wt.% lipids concentration on the 200 mesh copper grids covered with carbon film. Negative staining was applied by uranyl acetate with 0.5 wt.% concentration. The grids were dried at room temperature overnight.

Small angle X-ray scattering (SAXS). SAXS experiments were conducted at the 16ID-LiX Beamline station at the National Synchrotron Light Source II where is located at the Brookhaven National Laboratory (Upton, NY). The lipid concentration of pristine bicelle and **HP**-loaded bicelle is 1 wt.%. The standard flow-cell-based solution scattering was setup and the X-ray energy was 13.5 keV. The intensity is expressed as a function of scattering vector, q defined as $\frac{4\pi}{\lambda} sin\frac{\theta}{2}$, where θ is the scattering angle and λ is the wavelength. The data cover a q range from 0.005 to 2.5 Å^{-1}. Radial averaging and q-conversion of data were analyzed by using Jupyter Notebook.[5] The background subtraction and transmission correction were performed to minimize the intensity of the hydrogen bond from water at ~ 2.0 Å^{-1}.

Very small angle neutron scattering (vSANS). The vSANS measurements were taken on the **HP** in DMSO-d_6 with a concentration of 0.5 wt.% and **HP**-loaded deuterated-bicellar aqueous solution with a D_2O/H_2O volume ratio of 82.5/17.5 (lipid concentration of 1 wt.%). The vSANS setup at National Institute of Science and Technology (NIST) center for neutron research (NCNR, Gaithersburg, MD). The average wavelength of 5 Å was used with a spread of 12.5%. This yielded a q range from 0.024 $Å^{-1}$ to 0.8 $Å^{-1}$. The front and middle detectors were used for low and high q data collection, respectively. The 2D raw data were corrected by the detector sensitivity, background, scattering and transmission of empty cells and sample transmission. The corrected data were then circularly averaged, yielding 1D profiles and the intensity was put on the absolutely scale using the measured incident beam flux. The data reduction package was provided by NIST using the IGOR macros with IGOR Pro software.

Differential scanning calorimetry (DSC). DSC experiments were conducted using a NanoDSC (TA Instruments, New Castle, DE). The pristine bicelle and **HP**-loaded bicelle were diluted to 0.1 wt.%. The 0.5 mL of DI water and samples were loaded into the reference and sample cells, respectively. The pressure was kept at 3 atm (304 kPa) during the experiments. Before each measurement, samples were equilibrated at 30℃ for 10 minutes. The data was collected from 30 to 55 ℃ at the rate of 0.5 ℃ per minute and it was corrected for solvent background after measurements. The baseline was adjusted by using TA Instrument software.

SAXS MODELS

Scattering intensity, $I(q)$, of a particulate system can be expressed by the multiplication of volumetric concentration, c_{lp}, a contrast factor, $\Delta\rho^2$, form factor $P(q)$ and a structure factor $S(q)$ as

$$I(q) \propto c_{lp} \cdot \Delta\rho^2 \cdot P(q) \cdot S(q)$$

For SAXS data, 5-Layer Core Shell Discoidal (5LCSD) model[6] and Hayter-Penfold (MSA) model were used as the form factor and structure factor, respectively. The best fitting procedure was performed using SasView (https://www.sasview.org/)

Five-Layer Core Shell Discoidal (5LCSD) model. A 5LCSD model was previously developed to resolve the structural parameters from SAX data of bicelles. The form factor of 5LCSD model can be described as

$$P_{5LCSD}(q,\alpha) = \left[(\rho_{methyl} - \rho_{methylene}) V_{methyl} \frac{2J_1(qRsin\alpha)}{qRsin\alpha} \frac{\sin\left\{q\left(\frac{L_{methyl}}{2}\right)cos\alpha\right\}}{q\left(\frac{L_{methyl}}{2}\right)cos\alpha} + (\rho_{me}\right.$$

,

where ρ_{methyl}, $\rho_{methylene}$, ρ_s, ρ_r and ρ_{solv} are scattering length density (SLD) of methyl, methylene, shell and solvent, respectively. V_{methyl}, V_{c}, $V_{\text{c+s}}$ and V_{t} are the volume of methyl, core and core plus shell and thickness, respectively and $L = L_{\text{methyl}} + L_{\text{methylene}}$, where $L_{\text{methylene}}$ and L_{methyl} are the thicknesses of methylene and methyl groups, respectively. T_{s} and T_{r} are the thickness of shell and rim, respectively. J_1 is the first-order Bessel function of the first kind and α is the angle between the bilayer normal, q for averaging over the orientations and R is the core radius. The schematic of 5LCSD model is shown in Figure S1.

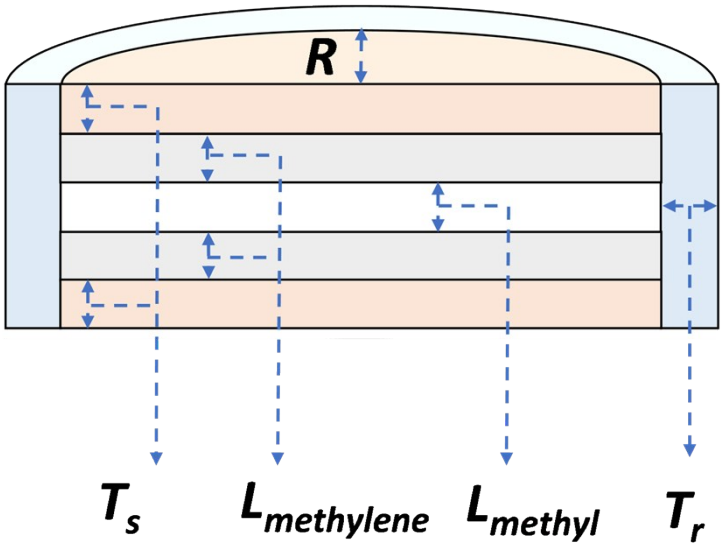

Figure S1. The schematic of Five-Layer Core Shell Discoidal (5LCSD) model.

Hayter-Penfold (MSA) model.[7, 8] The interaction of charged particles contributing to small angle scattering patterns can be described by Hatter-Penfold model, which accounts for the Coulombic interaction. The S(q) can be related to the approximated potential, $U(r)$. The repulsive potential between two identical spherical macroions of diameter σ is

$$U(r) = \frac{\pi\epsilon_0\epsilon\sigma^2\Psi_0^2\exp\left[-\kappa(r-\sigma)\right]}{r},$$

where r is the interionic center to center distance, ϵ is the dielectric constant of the solvent, Ψ_0 is the surface potential, ϵ_0 is the permittivity of free space. $1/\kappa$ is the Debye-Hückle length.

SANS MODELS

In the SANS experiments, the form factor model used for bicelle is core-shell discoidal model which can readily be used in SasView (https://www.sasview.org/).

Core Shell Discoidal model (CSD).[9, 10] The expression of the form factor, $F_{CSD}(q, \alpha)$ based on the schematic shown in Figure S2 is described as

$$I(q) = \frac{scale}{V_t}\int F_{CSD}(q,\alpha)^2 sin\alpha d\alpha + background$$

where $F_{CSD}(q, \alpha)$ represent the volume fraction of lipids and form factor of core-shell discoidal structure, respectively. The $F_{CSD}(q, \alpha)$ can be described as

$$P_{CSD}(q,\alpha) = \left[(\rho_{core} - \rho_{shell})V_c \frac{2J_1(qRsin\alpha)}{qRsin\alpha} \frac{\sin\left\{q\left(\frac{L}{2}\right)cos\alpha\right\}}{q\left(\frac{L}{2}\right)cos\alpha} + (\rho_{shell} - \rho_{rim})V_{c+s} \frac{2J_1}{}\right.$$

where ρ_{core}, ρ_{shell}, ρ_{rim} and $\rho_{solvent}$ are scattering length density of core, shell, rim and solvent, respectively. The V_c, V_{c+s}, and V_t are the volume of core, core plus shell of the disc and the whole disc, respectively. R, L, T_s and T_r are the core radius, thickness of the core, shell and rim, respectively. $J_1(qR\sin\alpha)$ is the first-order Bessel function of the first kind and α is the angle between the bilayer normal and q for averaging over all possible orientations.

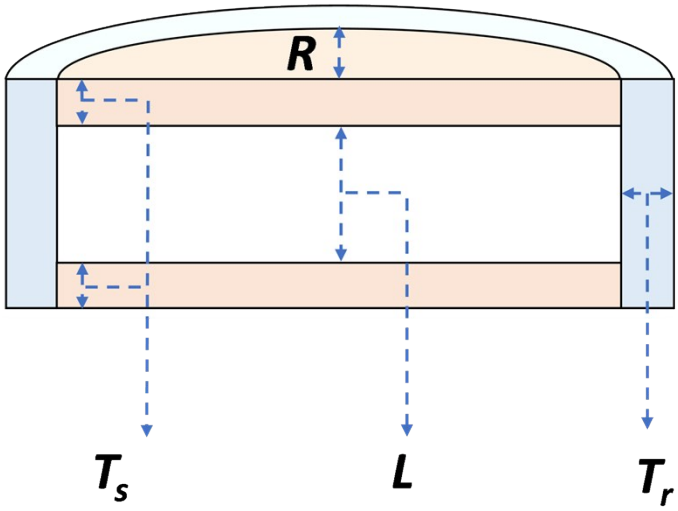

Figure S2. The schematic of core shells discoidal (CSD) model.

Core shell cylinder model (CSC).[11] The **HP** can be analyzed by using core shell cylinder model and SANS intensity, $I(q)$ can be described as

$$I(q) = \emptyset_{cylinder} \cdot P_{cylinder}(Q) = \emptyset \int_0^{\frac{\pi}{2}} \frac{g^2(q,\alpha)}{V_s} sin\alpha d\alpha,$$

where ϕ and $P(Q)$ are the volume fraction and form factor of cylinder and $g(q,\alpha)$ can be expressed as

$$g(q,\alpha) = 2(\rho_{core} - \rho_{shell})V_{core} \frac{sin(\frac{qL}{2}cos\alpha)}{\frac{qL}{2}cos\alpha} \cdot \frac{J_1(qRsin\alpha)}{qRsin\alpha} + 2(\rho_{shell} - \rho_{solvent})V \cdot \frac{J_1(Q(R+t)sin\alpha)}{q(R+t) \cdot sin\alpha}$$

where ρ_{core}, ρ_{shell}, and $\rho_{solvent}$ are scattering length density of core, shell and solvent, respectively. The V_{core} and V_t are the volume of core and total volume of cylinder, respectively. R and L are the core radius and length, respectively. The t is the thickness of shell. $J_1(qR\sin\alpha)$ is the first-order Bessel function of the first kind and α is the angle between the axis of the cylinder and scattering vector, q.

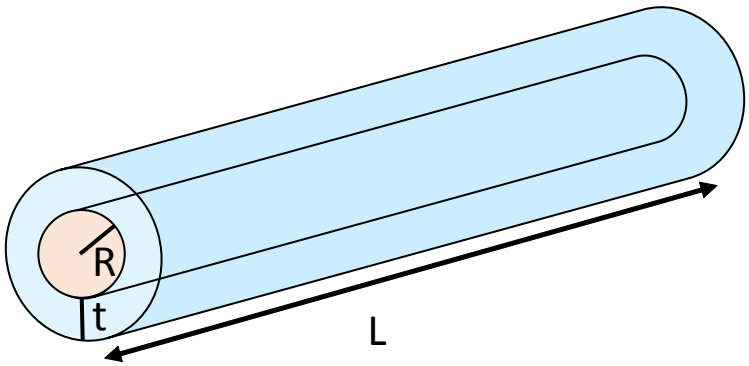

Figure S3. The schematic of core shell cylinder (CSC) model.

FIGURES AND TABLES

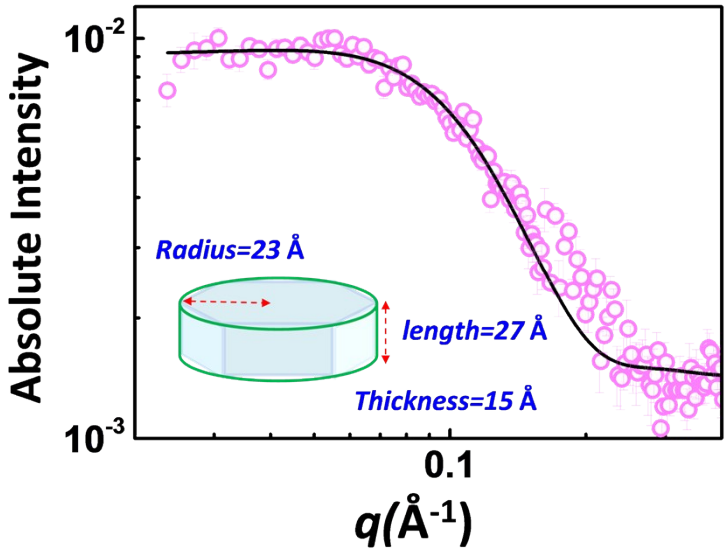

Figure S4. The vSANS data of free **HP** in DMSO. The hollow sphere shape and solid curve are the experimental data and best fit using the CSC model, respectively. Structural dimensions were in listed in Table S1.

Table S1. The best fitted vSANS results of free **HP** in the $CHCl_3$/MeOH mixture

best fitting parameters	**Values**
Radius (Å)	23 ± 3
Thickness (Å)	15 ± 5
Length (Å)	27 ± 4
$\rho_{core}(10^{-6}Å^{-2})$	3.2 ± 0.1
$\rho_{shell}(10^{-6}Å^{-2})$	5.50 ± 0.03

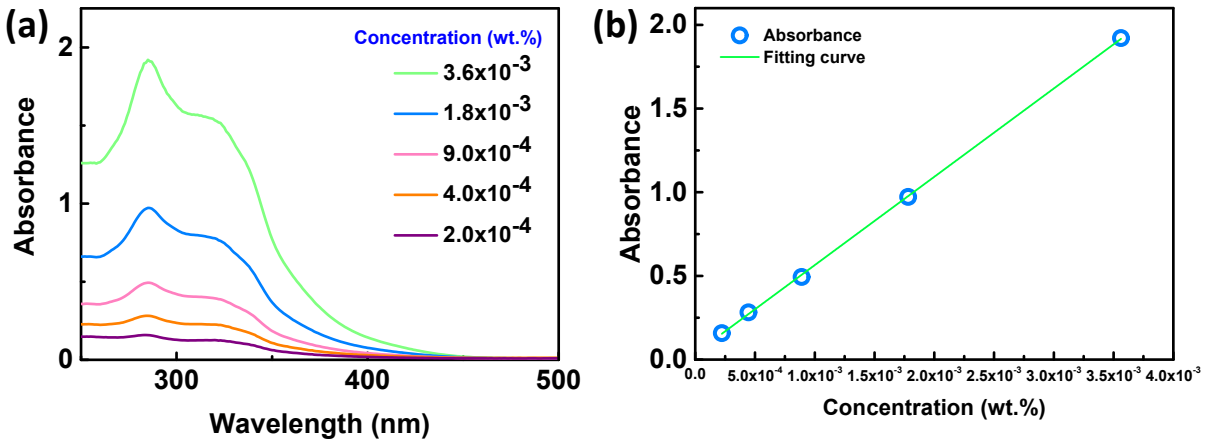

Figure S5. (a) The UV-vis absorption spectrum of free **HP** in the $CHCl_3$/MeOH mixture with different concentrations. (b) The absorbance peak (at 285 nm) versus concentrations (calibration curve).

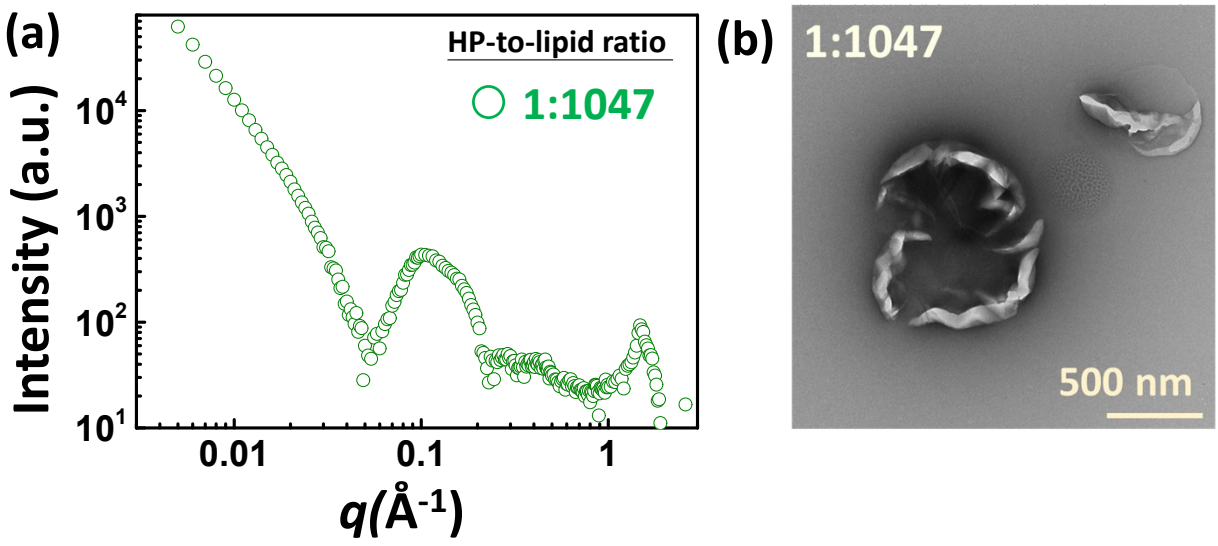

Figure S6. (a) The SAXS pattern and (b) TEM image of **HP**-to-lipid ratio 1:1047. A relatively sharp peak at ~ 0.1 Å^{-1} (on a broader peak) corresponds to the structure of multilamellar vesicles. TEM image also shows the broken fragments of vesicles.

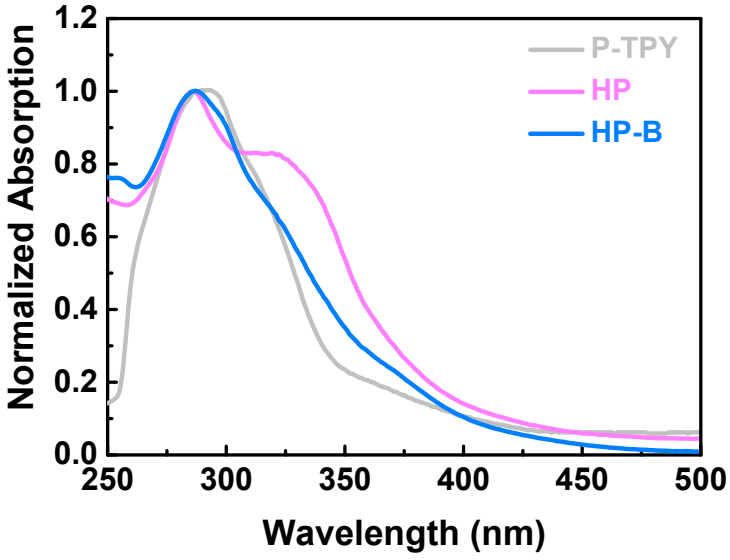

Figure S7. The UV-vis absorption spectra of P-TYP (a 2D-structure with less π–π interaction), free **HP** in $CHCl_3$/MeOH mixture and **HP-B**.

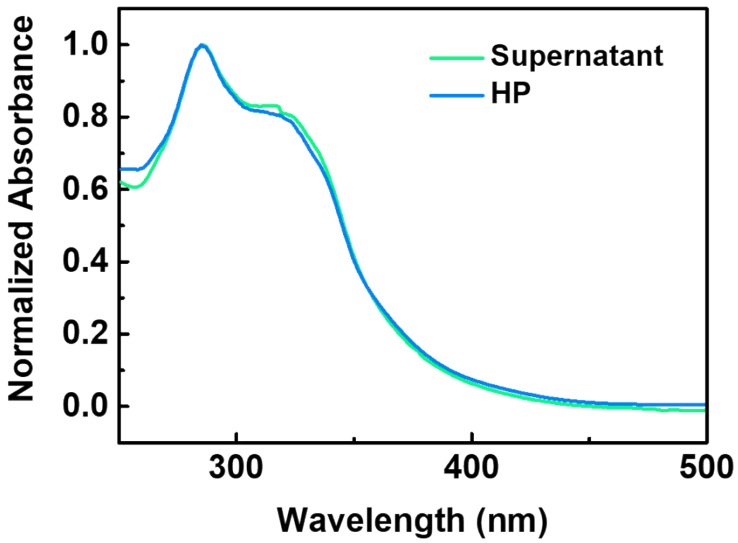

Figure S8. The UV-vis spectrum of re-dispersed sample of dried supernatant **HP-B** in the mixture of $CHCl_3$/MeOH as compared with that of the **HP** in the same solvent**.**

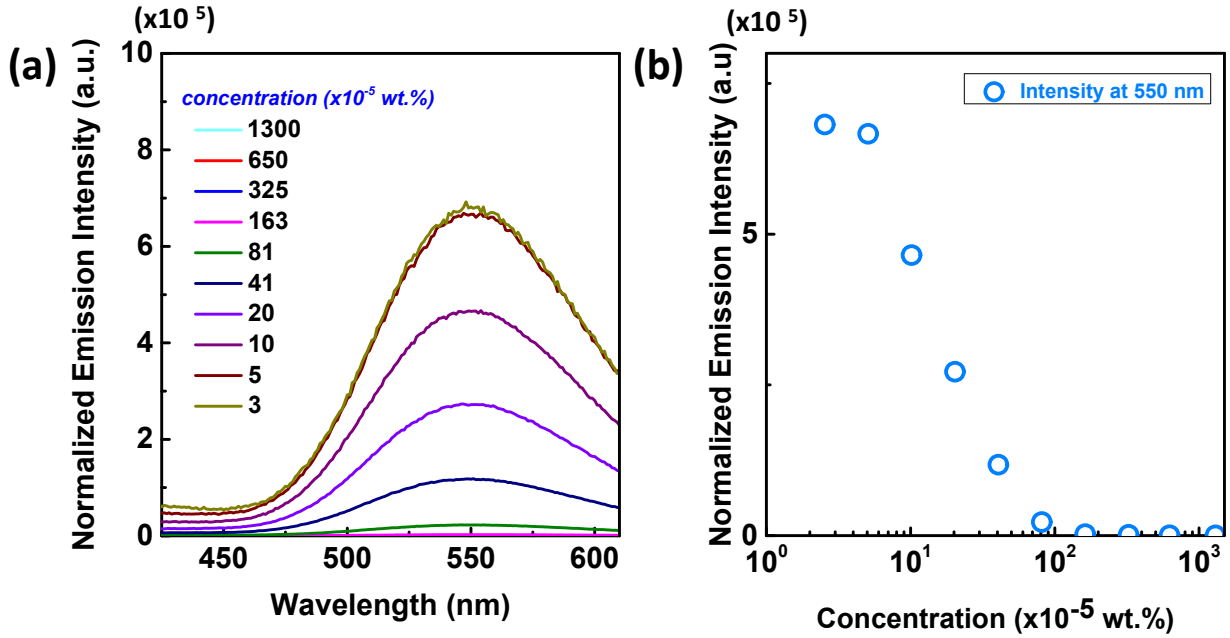

Figure S9. (a) The normalized fluorescence (λ_{ex}= 320 nm) of free **HP** in $CHCl_3$/MeOH mixture by **HP** concentration as a function of **HP** concentration from 1.3×10^{-2} to 2×10^{-4} wt.%. (b) The normalized emission peak intensity versus **HP** concentration on a semi-log plot for clarity.

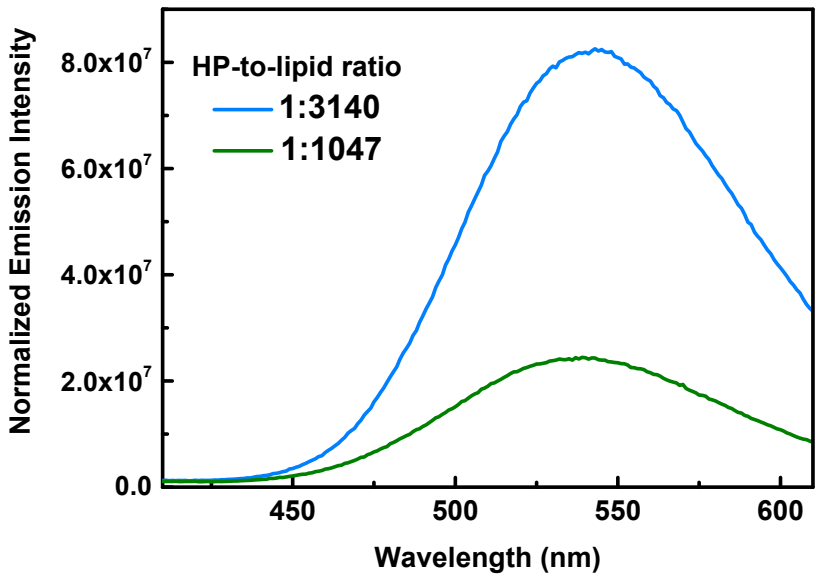

Figure S10. The normalized fluorescence of **HP**-to-lipid ratios of 1:3140 and 1:1047.

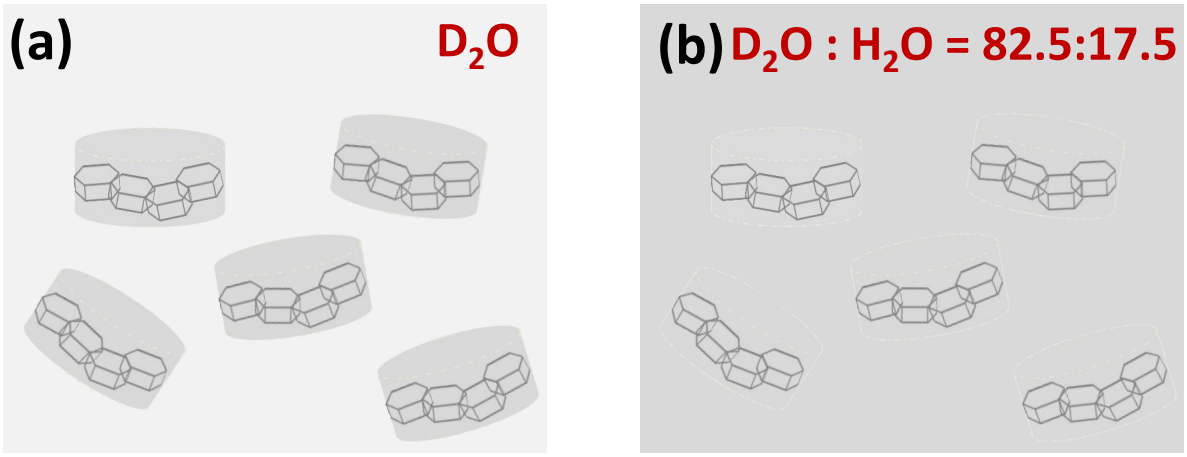

Figure S11. (a) The schematic of **HP-B** (proteated lipids) dispersed in D_2O. The scattering intensity is contributed by different contrast among solvent, lipids and **HP**. (b) Under the CM circumstances ($\rho_{solvent} = \rho_{lipid}$), the scattering contribution from the contrast between solvent and lipids are negligible and thus the location of **HP** can be obtained inside the bicelles.

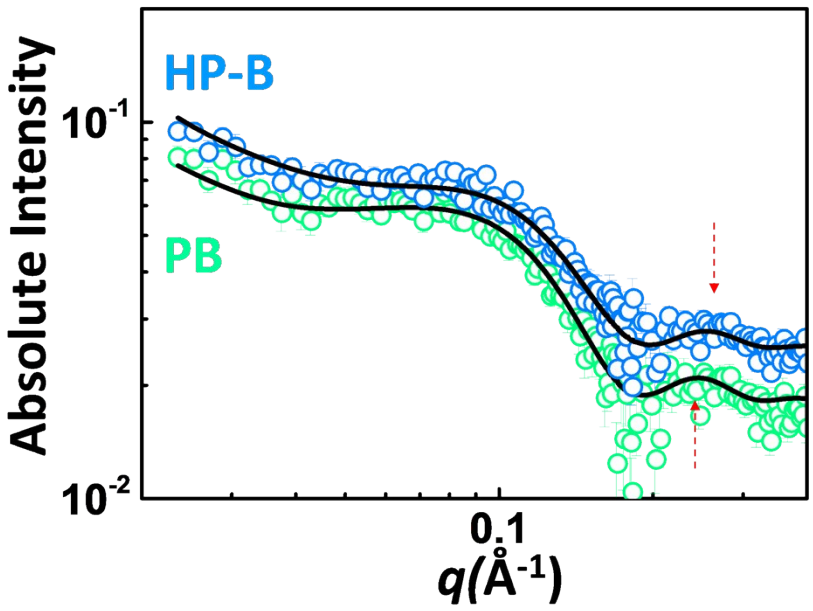

Figure S12. The vSANS results of **PB** and **HP-B** at the absolute scale. The best fits (solid curves) were analyzed by the CSD model.

Table S2. The best fitted results of **PB** and **HP-B**

Parameters /Samples	**PB**	**HP-B**
Core Radius (Å)	95 ± 11	208 ± 87
T_r *(Å)*	45 ± 5	94 ± 40
L_{length} *(Å)*	39 ± 0.4	37 ± 0.3
ρ_{core} *(× 10 $^{-6}$Å^{-2})*	7.25 ± 0.02	7.26 ± 0.14
ρ_{rim} *(× 10 $^{-6}$Å^{-2})*	5.05 ± 0.05	4.80 ± 0.14

Disclaim:

Access to vSANS was provided by the Center for High Resolution Neutron Scattering, a partnership between the National Institute of Standards and Technology and the National Science

Foundation under Agreement No. DMR-2010792. Certain commercial equipment, instruments, or materials (or suppliers, or software...) are identified in this paper to foster understanding. Such identification does not imply recommendation or endorsement by the National Institute of Standards and Technology, nor does it imply that the materials or equipment identified are necessarily the best available for the purpose.

Reference

1. H. Wang, C.-H. Liu, K. Wang, M. Wang, H. Yu, S. Kandapal, R. Brzozowski, B. Xu, M. Wang, S. Lu, X.-Q. Hao, P. Eswara, M.-P. Nieh, J. Cai and X. Li, *Journal of the American Chemical Society*, 2019, **141**, 16108-16116.
2. Y. Liu, Y. Xia, A. T. Rad, W. Aresh and M.-P. Nieh, in *Liposomes: Methods and Protocols*, ed. G. G. M. D'Souza, Springer New York, New York, NY, 2017, DOI: 10.1007/978-1-4939-6591-5_22, pp. 273-282.
3. J. Gao, Q. Li, W. Chen, Y. Liu and H. Yu, *ChemPlusChem*, 2014, **79**, 725-731.
4. P. Panwar, B. Pandey, P. C. Lakhera and K. P. Singh, *Int J Nanomedicine*, 2010, **5**, 101-108.
5. L. Yang, *Journal of Synchrotron Radiation*, 2013, **20**, 211-218.
6. C. Cheu, L. Yang and M.-P. Nieh, *Chemistry and Physics of Lipids*, 2020, **231**, 104945.
7. J. B. Hayter and J. Penfold, *Molecular Physics*, 1981, **42**, 109-118.
8. J.-P. Hansen and J. B. Hayter, *Molecular Physics*, 1982, **46**, 651-656.
9. P. Yang, T. Lin, Y. Hu and U. Jeng, *Chinese Journal of Physics*, 2012, **50**, 349-356.
10. D. Singh, 2008.
11. I. Livsey, *Journal of the Chemical Society, Faraday Transactions 2: Molecular and Chemical Physics*, 1987, **83**, 1445-1452.